

FACILE SYNTHESIS OF CUO/ITO FILM VIA THE CHRONOAMPEROMETRIC ELECTRODEPOSITION FOR NONENZYMATIC GLUCOSE SENSING

TRAN THI THUY DUONG^{1,2}, NGUYEN QUOC DUNG^{3,†}, TRAN DAI LAM^{2,4}
PHAM HONG CHUYEN³ AND NGUYEN TIEN DAI⁵

¹*Faculty of Basic Science -Thai Nguyen University of Agriculture and Forestry, Vietnam*

²*Graduate University of Science and Technology, VAST, 18 Hoang Quoc Viet, Hanoi, Vietnam*

³*Department of Chemistry, Thai Nguyen University of Education*

⁴*Institute for Tropical Technology, Vietnam Academy of Science and Technology, Vietnam*

⁵*Institute of Theoretical and Applied Research, Duy Tan University, Hanoi, 100000, Vietnam*

[†]*E-mail: dungnq@tue.edu.vn*

Received 3 February 2020

Accepted for publication 21 April 2020

Published 14 May 2020

Abstract. *We report on the synthesis of copper (II) oxide (CuO)/indium tin oxide (ITO) electrode via the electrochemical deposition method using a CuSO₄ solution and then thermal oxidation in air at temperature of 400°C for 2 h. The crystalline structure and morphology of CuO were characterized by scanning electron microscope (SEM), energy-dispersive X-ray spectroscopy (EDS), and X-ray diffraction (XRD). The electrochemical properties of the CuO/ITO electrode to glucose in the alkaline medium of 0.1 M NaOH solution were investigated by cyclic voltammetry (CV) and Chronoamperometry. The CuO-N/ITO electrode showed the best electrochemical properties for glucose detection in comparison to the others. Chronoamperometry of CuO-N/ITO electrode to the glucose response showed excellent stability, the linear range of 1 μM to 3600 μM with high sensitivity of 283.6 μAcm⁻²mM⁻¹ and 0.61 μM of the detection limit (S/N = 3). A good response of the CuO-N/ITO electrode, which was investigated for different human serum samples, indicates a high potential of its towards a glucose sensor for analysis in real examples.*

Keywords: copper (II) oxide, glucose sensing, chronoamperometry, cyclic voltammetry, human serum.

Classification numbers: 73.50.Pz; 81.15.Pq; 82.45.Qr.

I. INTRODUCTION

Glucose biosensors have been received much attention due to their importance in diabetes diagnosis, food industries, and environmental control [1–4]. The enzymatic glucose sensor, which was first demonstrated by Clark and Lyons [5] in 1962, has now developed to the third generation [6] with many advantages such as high sensitivity, good selectivity, and low detection limit. However, the enzyme is sensitive to temperature, pH , and toxic environment due to its intrinsic nature, resulting in the restriction of enzyme electrode applications [2–4]. For solving limitations, a fourth-generation biosensor with replacing enzyme electrodes by metallic electrodes as a glucose detector at low potential has been developed [7–9]. Noble metals (Pt, Au, Pd, etc.) have been investigated; however, these electrodes still have some drawbacks such as slow kinetics, poor selectivity, and effect by the poisoning of chloride ions [7,9]. Copper oxides with nano- and micro-structures [7,9–14] or composites using either graphene or carbon nanotubes or gold with copper, etc. [15–21] as non enzymatic electrodes for glucose determination have been recently interested because of its good characters such as wide response range, low detection limits, stability, and immunity to the poisoning of chloride ions.

The fabrication of CuO electrodes includes two steps: (1) the high dispersion of the starting material in a solvent and then (2) the adhesion of the starting material onto the substrate by techniques of embedding, spin-coating, and drop-casting [22–24]. The disadvantage of embedding and drop-casting techniques are weak repeatability and the non-uniform surface of the electrode. The spin coating method requires the substrate is square or circle; thus, it is not suitable to fabricate the electrode [22]. Directly deposition of Cu onto the substrate by the physical vapor deposition (PVD) and chemical vapor deposition (CVD) methods require high temperature, complicated equipment, expensive, and toxic [25–27]. Even though the sputtering method is conducted at low temperatures, the crystal structure of production is hard to control. Nevertheless, it is still quite challenging to ensure a facile and reproducible fabrication of CuO electrodes.

Therefore, in this work, we investigated the fabrication of the CuO/ITO electrode by a facile two-step process: (i) the Cu electrodeposition on the ITO substrate; (ii) the thermal oxidation to convert Cu to CuO. The as-synthesized CuO layer showed excellent adhesion on the ITO substrate, and the crystal structure of the as-synthesized CuO could be controlled by changing the electrolyte. The cyclic voltammetry was used to investigate the electrochemical properties of the CuO/ITO electrode to glucose in the alkaline medium of 0.1 M NaOH solution. Besides, for practical purposes, the CuO/ITO electrode was also tested with human serum samples.

II. EXPERIMENT

II.1. Reagents and Materials

D-glucose, sodium hydroxide, copper sulfate hexahydrate, sulfuric acid, and human serum were purchased from Sigma-Aldrich. All solutions were made using double distilled water. Prior to use, the indium tin oxide (ITO) substrate with a resistance of $6.5 \Omega/m^2$ and a size of $0.5 \text{ cm} \times 2.0 \text{ cm}$ (Samsung Corning Co. Ltd., Seoul Korea) was rinsed with methanol and acetone and then with double distilled water.

II.2. Preparation of the CuO thin film onto ITO substrate

Herein, the chronoamperometric deposition of CuO thin-film on ITO substrate was

conducted in two steps as follows: (i) Cu thin-film was deposited on the ITO substrate by electrochemical method; (ii) the conversion of Cu to CuO by calcination at temperature of 400°C in air. Three starting solutions for the preparation of Cu film were used: (1) 0.1 M CuSO₄ without supporting electrolyte; (2) 0.1 M CuSO₄ with a supporting electrolyte of 0.1 M H₂SO₄; and (3) 0.1 M CuSO₄ with a supporting electrolyte of 0.1 M Na₂SO₄. The applied potential was at -0.6 V (vs. Ag/AgCl reference electrode). The electrodes were fabricated using the starting solution №1, 2, and 3 were denoted as CuO-C/ITO, CuO-H/ITO, and CuO-N/ITO electrodes, respectively. Nonconductive epoxy was used to fix the electrode area of 0.5 cm × 0.5 cm.

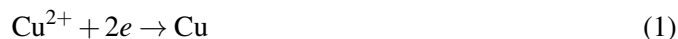
II.3. Structural characterization and electrochemical measurements

The structure, morphology, and elemental composition characterizations of the as-synthesized electrodes were investigated by X-ray diffraction (XRD, Bruker D8 Advance diffractometer) scanning electron microscope (SEM, Hitachi S-4800) equipped with energy-dispersive X-ray spectroscopy (EDS). The potentiostat & Galvanostat instrument (Autolab 302N) controlled by the Nova 1.10 software was used for electrochemical measurement in the three-electrode system. A fabricated electrode served as the working electrode, while a Ag/AgCl|Cl (saturated KCl) electrode and Pt sheet were used for the reference and the counter electrodes, respectively. The cyclic voltammetry (CV) was used to study the electrochemical properties of the fabricated electrode. The quantification of the glucose concentration in the solution was investigated by the chronoamperometric method. To test the applicability for practical purposes, human serum samples were also prepared to determine glucose using the CuO-N/ITO electrode.

III. RESULTS AND DISCUSSION

III.1. Copper deposition

Cyclic voltammograms (C.V.s) were employed to study the response of 0.1 M CuSO₄ solution with a scan rate of 20 mV/s under different supporting electrolytes. The effect of electrolyte supports cyclic voltammetry (from +0.6 V to -0.9 V, the scan rate of 20 mV/s) of the ITO electrode in 0.1 M CuSO₄, as shown in Fig. 1. There was no current, initially, the potential of -0.019; -0.113; -0.022 V was reached in solution of 0.1 M CuSO₄ (solution 1); 0.1 M CuSO₄ + 0.1 M H₂SO₄ (solution 2) and 0.1 M CuSO₄ + 0.1 M Na₂SO₄ (solution 3), respectively. At this voltage, the cathodic current started to increase and form peak I_c (for solution 2 and 3) at a potential that depended on the electrolyte support as following reaction (1):



In the case of solution №1, I_c peak (cathodic current peak) presents that was not electrolyte support. For the solutions, №2 and 3, the decaying cathodic current past the peak I_c with a potential of -0.474 V and -0.411 V, respectively obeys diffusion-controlled regime [28]. In reverse scan, the anodic current appeared and had an I_a peak (anodic current peak) with a potential of 0.362 V, 0.366 V, and 0.440 V for solutions №1, 2, and 3, respectively, that was related to oxidation of Cu formation in a forward scan. All of CuO/ITO electrodes were fabricated using electrodeposition by the chronoamperometry method in 120 seconds at an applied potential of -0.6 V (the current value was steady, as seen in Fig. 1) followed by the oxidation of Cu at temperature of 400°C in air.

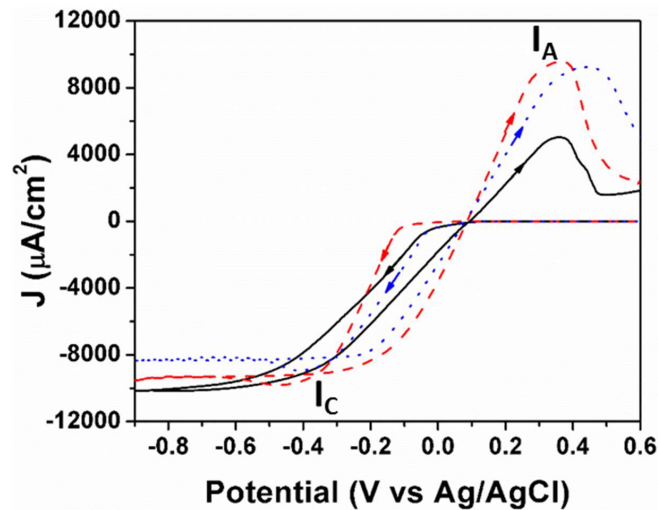


Fig. 1. Cyclic voltammograms (C.V.s) of CuSO_4 under different electrolyte solutions. black curve: no supporting electrolyte, blue dot curve: supporting electrolyte of 0.1 M H_2SO_4 and red dash curve: supporting electrolyte of 0.1 M Na_2SO_4 .

III.2. Structure and characterization

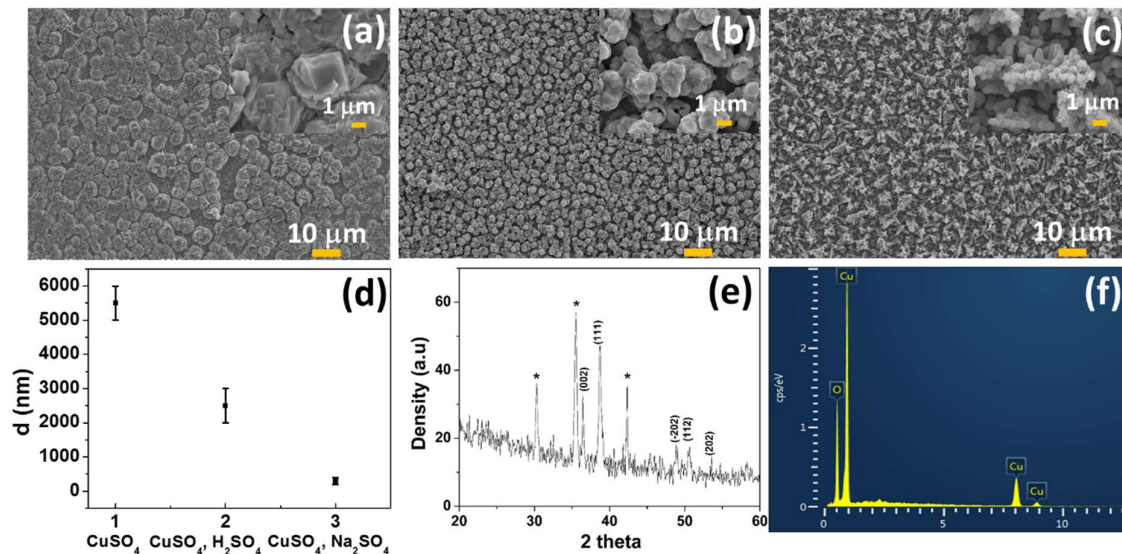


Fig. 2. SEM image of a) CuO-C, b) CuO-H, c) CuO-N, d), e) XRD pattern of CuO-N/ITO and (f) EDS analysis of CuO-N/ITO electrode.

Figure 2 presents SEM images of the CuO layer deposited on the ITO substrates. As a result, the starting solution considerably altered the morphology of CuO. In Fig. 2(a), the as-prepared

Cu morphology shows a sphere-like structure with particle size in a range of 5–6 μm while used only 0.1 M CuSO_4 solution. Spherical CuO was also observed in CuO-H/ITO (Fig. 2(b)) and CuO-N/ITO (Fig. 2(c)) electrodes, but their particle size is smaller than that of CuO-C, implying that the supporting electrolyte could influence the formation of CuO crystalline particles. The particle size of CuO-H and CuO-N are in the range of 3–4 μm and 300–500 nm, respectively. The smallest size of CuO-N promised the best sensitivity of the CuO-N/ITO electrode in comparison with CuO-C/ITO and CuO-H/ITO electrodes. This excellent response is assigned to a higher electrochemical activity area when CuO particle size is smaller. Fig. 2(e) shows the XRD pattern of CuO-N on the ITO substrate with 2θ diffraction peaks at 35.4° , 38.5° , and 48.9° , indicating the monoclinic phase of CuO (JCPDS №045-0937). Fig. 2(f) shows EDS analysis of CuO-N sample, in which the atom ratio of O and Cu is roughly determined to be 55:45 in accordance with 1:1 ratio of O and Cu in CuO. However, the atom ratio of O is higher than that of Cu, which is attributed to the adsorption of oxygen on the CuO surface or the presence of $\text{Cu}(\text{OH})_2$, which is caused by the exposure of CuO surface to the environment moisture.

III.3. Electrochemical properties

III.3.1. Selection of the supporting electrolyte in CuO/ITO electrode

Figure 3 shows the cyclic voltammogram of CuO-C/ITO, CuO-H/ITO, and CuO-N/ITO electrodes measured in 0.1 M NaOH in the absence (black line curve) and presence (red dot curve) of 1mM glucose. Fig. 3(c) displays a glucose oxidation peak of +0.52 V and one more small peak of +0.60 V in the presence of 1 mM glucose. In contrast, the unclear peak appeared for CuO-C/ITO and CuO-H/ITO electrodes that proved slow-kinetic of these electrodes in comparison with the CuO-N/ITO electrode. It is exciting after the background subtraction of cyclic voltammogram of electrodes by subtraction between CV signal of positive scan measured in NaOH solution with glucose and without glucose shows in Fig. 3(c). The faradaic current of glucose response was evident, with an oxidation peak at the potential of 0.52 V. Thus, subtracted C.V.s current can be used to appraise the electrochemical properties of the electrodes. We can see the highest glucose response and the lowest glucose oxidation peak (+0.52 V) of the CuO-N/ITO electrode in comparison to the CuO-C/ITO electrode (+0.63V) and the CuO-H/ITO electrode (+0.61V). For further study, the CuO-N/ITO electrode was selected.

III.3.2. Chronoamperometric detection to glucose of CuO-N/ITO electrode

Based on the cyclic voltammogram of the CuO-N/ITO electrode, as shown in Fig. 3(c), even though the current peak of glucose oxidation was about +0.52 V (vs. Ag/AgCl), for further studies, we selected a slightly lower potential, at 0.45 V, for chronoamperometric measurement, to avoid the possible interference as in Ref. [2].

We utilized the chronoamperometric technique to quantify the glucose concentration in the solution in which a glucose oxidation potential was fixed, and the glucose oxidation current decayed versus time was recorded by Cottrel equation:

$$i = \frac{nFAC^0\sqrt{D}}{\sqrt{\pi t}} \quad (2)$$

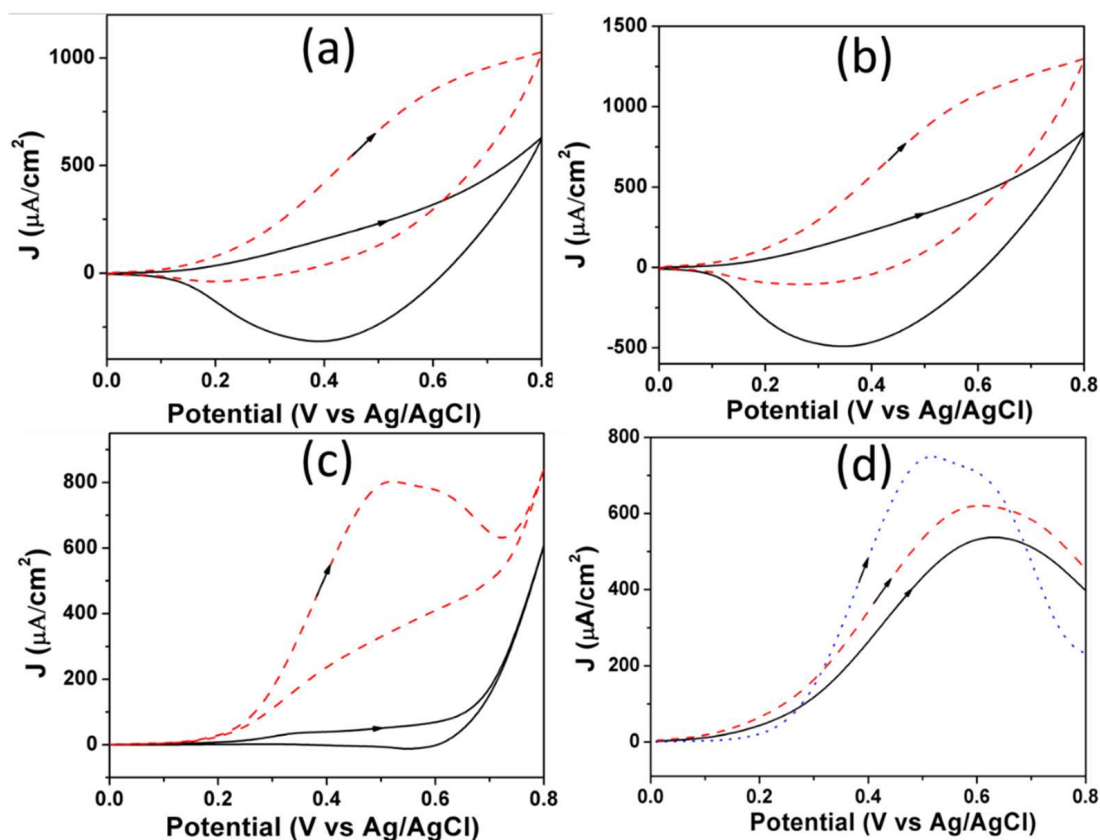


Fig. 3. Cyclic voltammograms of CuO-C/ITO (a), CuO-H/ITO (b), and CuO-N/ITO (c) electrodes in the absence (black line curve) and presence (red dot curve) of 1mM glucose; Background subtracted current of a positive scan of the electrodes for 1.0 mM glucose response (d).

where i is an electric current of the electrode with an area of A in the solution of analytical of C° versus time t , diffusion coefficient D , and Faraday constant F .

$$i = k.t^{-1/2} \quad (3)$$

where k is the collection of constants for a given system (n , F , A , C° , D).

Figures 4(a-c) shows the chronoamperometric measurement with CuO-N/ITO electrode in a 0.1 M NaOH solution at 0.45 V (vs. Ag/AgCl) with different glucose concentrations ranging from 0 μM to 10 μM in Fig. 4(a), from 0 μM to 100 μM in Fig. 4(b) and from 0 μM to 600 μM in Fig. 4(c), more specific concentrations are not shown. The calibration curve of oxidation current density [(after 35 seconds of chronoamperometry curve, as shown in Figs. 4(a-c)] versus the glucose concentration in Fig. 4(d) exhibited linearity for glucose sensing in the range from 1 μM to 3600 μM with a correlation coefficient (R) of 0.9998. According to the linear range, the

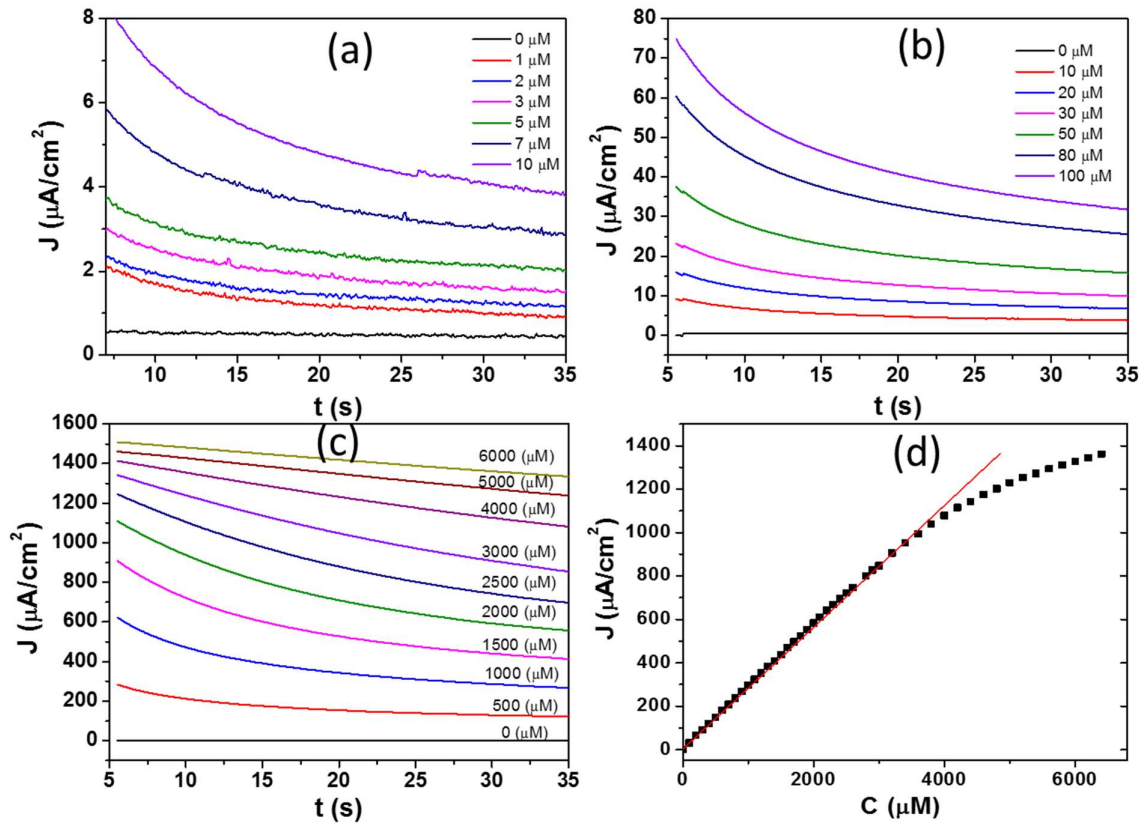


Fig. 4. The chronoamperometric response of CuO-N/ITO electrode at 0.45 V (vs. Ag/AgCl) to different glucose concentration scale (a) 0 μM to 10 μM ; (b) 0 μM to 100 μM ; (c) 0 μM to 6000 μM and (d) the calibration curve of dependence of the oxidation current density (after 35 s) on glucose concentration.

slope of the calibration curve indicated the sensitivity ($283.6 \mu\text{Acm}^{-2}\text{mM}^{-1}$) of the electrode and detection limit of $0.61 \mu\text{M}$ (an estimate of signal to noise equals 3).

Additionally, the electrochemical response of the CuO-N/ITO electrode was investigated in solution containing of individual interfering species such sucrose, ascorbic acid (AA), and uric acid (UA) by applying of oxidation potential at 0.45 V. Fig. 5 shows the specificity of the electrode by adding sucrose, UA, and AA of $50 \mu\text{M}$ in 0.1 M NaOH solution containing $500 \mu\text{M}$ glucose. The additional signals obtained as 0.75%, 6.63%, and 3.86%, for sucrose UA, and AA, respectively. Since the concentrations of the AA, and UA in the blood were 30 times less than glucose [2], the CuO-N/ITO electrode can be applied to determine glucose in human blood.

III.3.3. Application of electrode in the human serum sample

The CuO-N/ITO sensor electrode was investigated for human serum samples. The sample was prepared using water/or glucose mixing human serum samples to make different glucose concentrations. A human serum solution of $100 \mu\text{L}$ was diluted in a 25 mL 0.1 M NaOH solution.

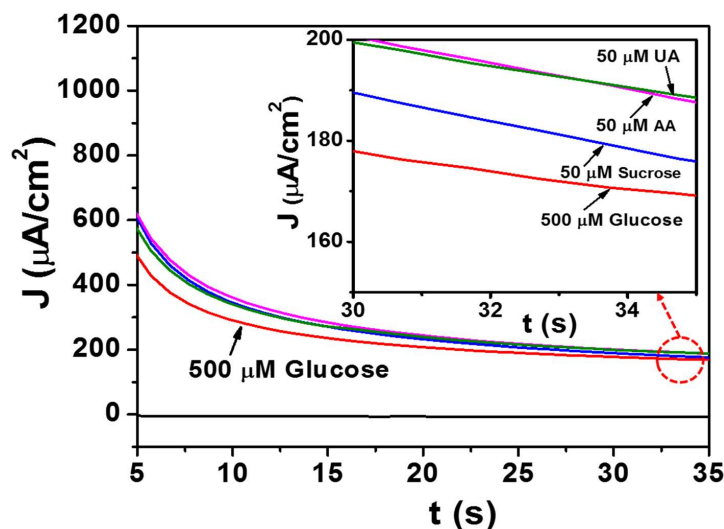


Fig. 5. The selectivity of CuO-N/ITO electrode was examined by measuring responses to interfering species of sucrose, AA and UA at an applied potential of 0.45 V in 0.1 M NaOH.

The chronoamperometric response was recorded at a potential of 0.45 V that was shown in Fig. 6. The solid black line and red dash line are corresponding to before and after adding the human serum sample, respectively. Based on the calibration curve (Fig. 4(d)), we calculated the glucose concentration and compared it with the prepared concentration listed in Table 1. The results indicate that the sensor is comparable with a commercial one (measured by RGII glucose meter), and the CuO-N/ITO electrode would be a useful approach for the development of non enzymatic glucose sensors for real samples.

Table 1. Comparison of CuO-N/ITO with RG II meter.

Samples	Glucose concentration by RG II* meter (mM)	Glucose conc. measured by CuO-N/ITO (mM)	Deviation (%)
1	4.91	5.41	10.2
2	7.76	8.01	5.0
3	9.73	9.84	1.2
4	15.42	16.94	9.9

* Glucose meter from Sejong Biotechnology (Korea)

Furthermore, the stable response of CuO-N/ITO electrodes for two months with 0.1 mM glucose were investigated. The current density response of the electrodes showed a negligible change due to the high stability of the CuO phase in a glucose solution. This result suggests another approach for fabricating the stable, selective non enzymatic glucose sensor.

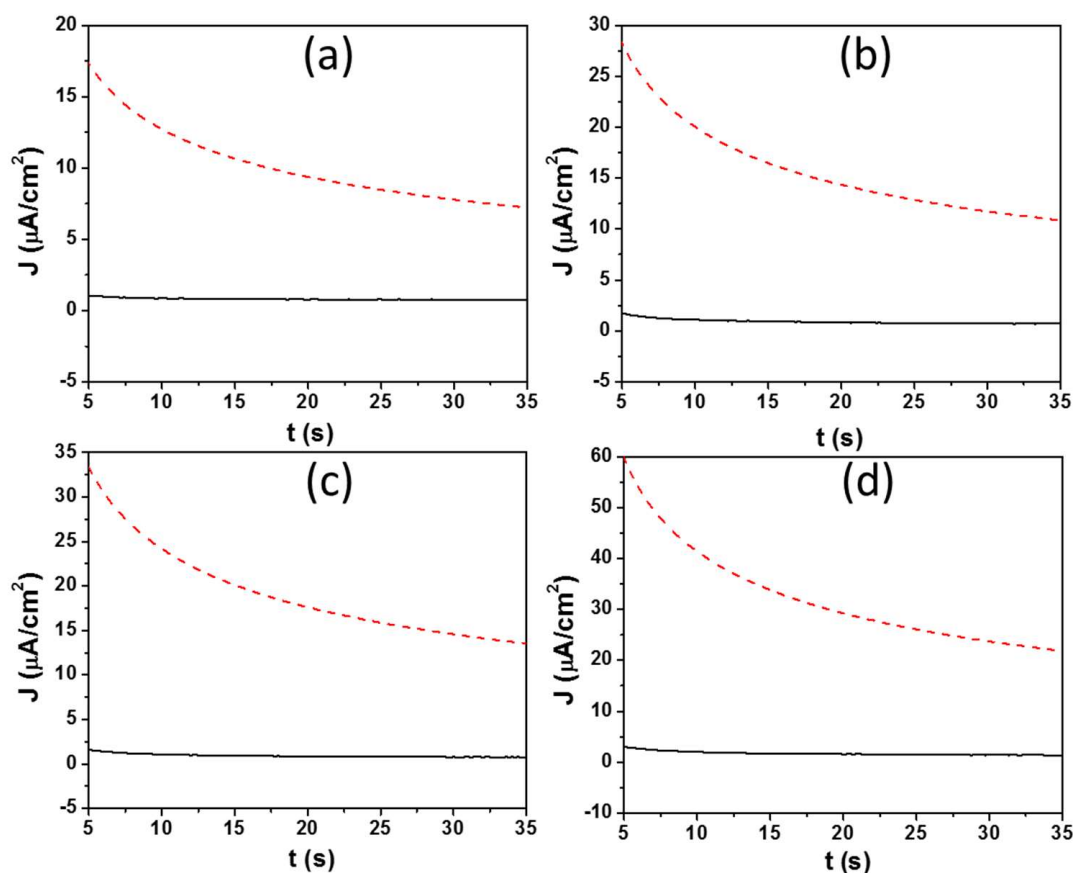


Fig. 6. The sensor was used for investigating human serum samples by the chronoamperometric method by adding 200 μL human serum sample to 250 mL 0.1 M NaOH solution at 0.45 V (vs. Ag/AgCl) with different glucose concentrations (a) 4.91 mM; (b) 7.71 mM; (c) 9.73 mM and (d) 15.42 mM. The solid black line and red dash line are before and after adding the human serum samples.

IV. CONCLUSION

We successfully applied the electrochemically deposited method to the synthesis of the Cu/ITO electrode, followed by an oxidation process at temperature of 400 $^{\circ}\text{C}$ in air to fabricate the CuO/ITO electrode for glucose sensing. In terms of the electrode: CuO-C/ITO, CuO-H/ITO, and CuO-N/ITO, we found out that the CuO-N/ITO electrode is the best for glucose sensing by investigating the cyclic voltammetry method. The CuO-N/ITO electrode for glucose determination using the chronoamperometric method showed a linear range of 1 μM to 3600 μM with a sensitivity of 283.6 $\mu\text{Acm}^{-2}\text{mM}^{-1}$ and detection limit of 0.61 μM . The CuO-N/ITO electrode was also investigated with a human serum sample indicated a high potential towards a commercial section of the non enzymatic glucose sensor.

ACKNOWLEDGMENT

This research is funded by Vietnam National Foundation for Science and Technology Development (NAFOSTED) under grant number 103.02-2016.63.

REFERENCES

- [1] N.Q. Dung, D. Patil, T.T. Duong, H. Jung, D. Kim, S.G. Yoon, *Sensors Actuators B Chem.* **166–167** (2012) 103.
- [2] N.Q. Dung, D. Patil, H. Jung, D. Kim, *Biosens. Bioelectron.* **42** (2013) 280.
- [3] N.Q. Dung, D. Patil, H. Jung, J. Kim, D. Kim, *Sensors Actuators B Chem.* **183** (2013) 381.
- [4] N.Q. Dung, T.T.T. Duong, T.D. Lam, D.D. Dung, N.N. Huy, D. Van Thanh, *J. Electroanal. Chem.* **848** (2019) 113323.
- [5] L.C. Clark, C. Lyons, *Ann. N. Y. Acad. Sci.* **102** (1962) 29.
- [6] M. Viticoli, A. Curulli, A. Cusma, S. Kaciulis, S. Nunziante, L. Pandolfi, F. Valentini, G. Padeletti, *Mater. Sci. Eng. C* **26** (2006) 947.
- [7] K.M. El Khatib, R.M.A. Hameed, *Biosens. Bioelectron.* **26** (2011) 3542.
- [8] Y. Wei, Y. Li, X. Liu, Y. Xian, G. Shi, L. Jin, *Biosens. Bioelectron.* **26** (2010) 275.
- [9] B. Yuan, C. Wang, L. Li, S. Chen, *Electrochem. Commun.* **11** (2009) 1373.
- [10] L.C. Jiang, W.D. Zhang, *Biosens. Bioelectron.* **25** (2010) 1402.
- [11] X. Liu, L. Long, W. Yang, L. Chen, J. Jia, *Sensors Actuators B. Chem.* **266** (2018) 853.
- [12] G. He, L. Wang, *Can. J. Anesth.* **24** (2018) 3167.
- [13] R. Li, X. Liu, H. Wang, Y. Wu, K.C. Chan, Z. Lu, *Electrochim. Acta* **299** (2019) 470.
- [14] M.S. Jagadeesan, K. Movlaee, T. Krishnakumar, S.G. Leonardi, G. Neri, *J. Electroanal. Chem.* **835** (2019) 161.
- [15] X. Xiao, H. Li, Y. Pan, P. Si, *Talanta.* **125** (2014) 366.
- [16] S. Yang, G. Li, D. Wang, Z. Qiao, L. Qu, *Sensors Actuators B Chem.* **238** (2017) 588.
- [17] D. Jiang, Q. Liu, K. Wang, J. Qian, X. Dong, Z. Yang, X. Du, B. Qiu, *Biosens. Bioelectron.* **54** (2014) 273.
- [18] M. Saraf, K. Natarajan, S.M. Mobin, *Dalt. Trans.* **45** (2016) 5833.
- [19] T.K. Huang, K.W. Lin, S.P. Tung, T. M. Cheng, I.C. Chang, Y.Z. Hsieh, C.Y. Lee, H.T. Chiu, *J. Electroanal. Chem.* **636** (2009) 123.
- [20] Q. Liu, Z. Jiang, Y. Tang, X. Yang, M. Wei, M. Zhang, *Sensors Actuators B Chem.* **255** (2018) 454.
- [21] M. Figiela, M. Wysokowski, M. Galinski, T. Jesionowski, I. Stepniak, *Sensors Actuators B Chem.* **272** (2018) 296.
- [22] C. Y. Chiang, K. Aroh, N. Franson, V. R. Satsangi, S. Dass, S. Ehrman, *Int. J. Hydrogen Energy.* **36** (2011) 15519.
- [23] C.Y. Chiang, Y. Shin, K. Aroh, S. Ehrman, *Int. J. Hydrogen Energy* **37** (2012) 8232.
- [24] S. M. Cha, G. Nagaraju, S. C. Sekhar, J. S. Yu, *J. Mater. Chem. A.* **5** (2017) 2224.
- [25] C. R. Crick, I. P. Parkin, *J. Mater. Chem.* **21** (2011) 14712.
- [26] Z.Y. Tian, H.J. Herrenbrück, P. M. Kouotou, H. Vieker, A. Beyer, A. Gölzhäuser, K. Kohse-Höinghaus, *Surf. Coatings Technol.* **230** (2013) 33.
- [27] A. Kowalik-Klimczak, E. Stanisławek, J. Kacprzyńska-Gołacka, B. Kaźmierczak, P. Wieciński, *J. Mach. Constr. Maintenance Probl. Eksploat.* **3** (2018) 49.
- [28] D. Grujcic, B. Pesic, *Electrochim. Acta* **47** (2002) 2901.